QSAR Modeling of α-Ketooxazole Motif Analogues as Potent Anti-Alzheimer Agents

Smita Jain[a], Neha Chauhan[a&b], Abhay Bhardwaj[c], Giriraj Yadaw[d&e], Mukesh Kr. Singh[f], Achal Mishra[g]

[a]Department of Pharmacy, Banasthali Vidyapith, Banasthali-304022, Rajasthan, India
[b]Department of Bioscience and Biotechnology, Banasthali Vidyapith, Banasthali-304022, Rajasthan, India
[c]Department of Pharmacy, KIET School of Pharmacy, Ghaziabad-201206, Uttar Pradesh, India
[d]Department of Chemistry, Banasthali Vidyapith, Banasthali-304022, Rajasthan, India
[e]NPD, Patanjali Ayurved Ltd., Patanjali Food and Herbal Park, Padartha, Haridwar-249404, Uttarakhand, India
[f]Department of Pharmaceutics, School of Pharmaceutical Sciences, IFTM, University, Moradabad-244102, Uttar Pradesh,India
[g]Shri Shankaracharya Technical Campus, Bhilai-490020 Chhattisgarh, India

***Corresponding author**
Achal Mishra
Shri Shankaracharya Technical Campus, Bhilai-490020 Chhattisgarh, India
Email id: achal.mishra03@gmail.com

Abstract
Studies of quantitative structure-activity relationships are undeniably important in computational chemistry. QSAR were performed on a series of 35 α-ketooxazole analogues searching for improved anti-Alzheimer agents. PLS (Partial least square), MLR (Multiple linear regression) and FFNN (Feed forward neural network) were used to develop the models, including different descriptors such as electronic, lipophilic, and topological. The statistical significance and prediction capability of QSAR models were assessed. f = 34.2924, s = 0.406483, r= 0.922545, r^2cv = 0.802496, r^2 = 0.849 are the best MLR statistical expressions with strong prediction and authentication capability. MLR, PLS, and FNN have r^2 (training and test-set) values of 0.8493, 0.8003, 0.8008, 0.763, 0.8577, and 0.8075, correspondingly, which indicate the model's soundness. The model indicates that the Kier chi 5 ring index, VAMP Heat of formation (whole molecule), and VAMP LUMO (whole molecule) greatly contribute to determining the anti-Alzheimer activity of FAAH (fatty acid amide hydrolase enzyme) antagonist. FAAH enzyme antagonists with increased potency as anti-Alzheimer agents may be developed using the model used in this work.
Keywords: *Lipinski's rule of five, Descriptors, fatty acid amide hydrolase, Alzheimer disease and Quantitative structure activity relationship*

Introduction

Alzheimer's disease (AD) is the commonest neurodegenerative disease, and its incidence rises with as life expectancy increases. However, histopathological markers, including amyloid β(Aβ) deposits[1], tau protein aggregation[2], and inflammation, oxidative stress, and acetylcholine dysfunction (ACh) signaling in the basal forebrain appear to play important roles even if their AD causes are not entirely recognized. Indeed, evidence of selective loss of presynaptic cholinergic neurons in Alzheimer's patients result in the introduction of cholinesterase inhibitors (ChEI) decades ago[3,4]by suppressing butyrylcholinesterase (BuChE) and acetylcholinesterase (AChE), enzymes that reduce ACh, the quantity of ACh in the neuronal synaptic cleft was temporarily raised. BuChE has gotten more attention in recent years because, as Alzheimer's disease develops, AChE activity declines, but BuChE activity rises, making it easier to quantify ACh concentrations in cholinergic neurons. As a result, both enzymes are therapeutic targets at various phases of pathology: mild to moderate and moderate to severe types of Alzheimer's disease.[5,6]

While decades-long efforts have been made in this field, the management of AD remains an area of major unmet requirement, with treatments that focus on the donepezil (donepezil), galantamine (galantamine), and ChEI (rivastigmine), except for memantine, an NMDA receptor antagonist.The symptoms of the condition are not altered by these medications, though.[7,8]

Recent years have seen the development of innovative techniques in medicinal chemistry to fulfil the growing need for AD-modifying medicines. Recently, it was suggested that one factor may not be enough to achieve the desired performance because of AD's multi-factorial and complicated etiology. Structures that may concurrently interact with various pathogenic targets are already being designed by researchers.[9]

The endocannabinoid system (eCB) is also being studied for Alzheimer's disease.[3,10] The eCB system comprises two G-protein-coupled receptors, CB_1 and CB_2, that bind to lipid signalling molecules: When activated, microglia in the AD brain are more likely to produce CB_2 receptors, which may be due to their inflammatory nature, while CB_1 receptors are typically present in neurons.[11] The presence of CB_2 receptors in certain areas of neuritic plaques shows that this receptor is involved in managing the inflammation associated with Alzheimer's disease. CB_2 receptor expression, in particular, might be an adaptive response to severe inflammation caused in Aβ-deposition sites to lower astrocyte and microglia activation. Also, the enzyme FAAH enhanced activity was exclusively observed in areas of Aβ-enriched neuritic plaques.[12] FAAH is a key membrane enzyme that catalyses the hydrolysis of various endogenous lipid messengers, such as eCBs; hence, inhibitors of FAAH would enable regulation of eCB signalling and increase neuronal transmission and counteract neuroinflammation, correspondingly, through CB_1 and CB_2 receptors. As a result, it was shown that inhibiting eCB inactivation early on reduced Aβ-induced gliosis, memory loss, and neuronal death.[13]Furthermore, the latest study has shown that anandamide levels are deficient in cortical parts of postmortem AD brains. These levels are associated directly with

the patients' positive cognitive scores and has a negative correlation with $A\beta_{42}$ accumulation.[14]

Due to experimental methodologies' time and expense constraints, computer-aided drug design, i.e., ligand- and structure -based approaches, has been widely utilized in the current drug discovery arena to search for new compounds. This may be utilized to forecast the endpoints of inquisitiveness in organic compounds that serve as medications in the drug discovery domain.[15,16] In terms of descriptors, a QSAR (quantitative structure-activity relationship) is a quantitative association of biological activity in the chemical compound structure.

The main objective of the investigation is to determine structural elements of α-ketooxazole motif derivatives fatty acid amide hydrolase inhibitor (FAAH) enhancing the anti-Alzheimer activity from the computationally derived molecular descriptors and the effectiveness of cannabinoid receptor-targeting neural networks in treating Alzheimer's disease will be evaluated.

Material and methods

The data used in this study are FAAH enzyme inhibitor activities of a set of 35 α-ketooxazole derivatives obtained from the literature.[17,18] The entire α-ketooxazole derivatives structures were built using ChemDraw Professional 15.1 software (Tables 1 and 2).

Due to the great variability in biological activities, many substitutes, and the fact that biological activities are extremely susceptible to skewed, all of the substitutions on the standalone module of Accelrys Discovery Studio (version 2.0) must be negative algorithmic scale. QSAR analysis was then carried out using the (inhibitory-constant) values indicated above as dependent variables (negative log IC_{50} values). Research on the TSAR software was carried out in more detail (version 3.3Accelrys Inc., Oxford, UK). All mol files are imported into the TSAR spreadsheet.

The series featured two significant substitutions specified in the TSAR worksheet's toolbar using the "define substituent" option.This step is also required when utilizing the Charge 2 generate charges option since the alignment of structures as per the molecular weight is required during optimization of a 3D structure.

Using the "Corina-make3D" option (developed by Rudolph, Gasteiger, and Sadowski)[19],the 2D molecules and substitutions that had been imported were transformed into their 3D structure. All 3D models were optimized using the "Cosmic-Optimize 3D" function, which contains valence terms like bond angles, bond potentials, non-bonded, and torsional potential variables like Vander Waals interaction and electrostatic interaction.

Table 1. Structure and biological activity data of α-ketooxazolemotif derivative analogues used in QSAR analysis

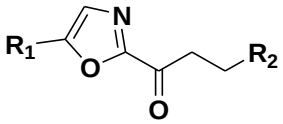

Compound	Substituents R1	Substituents R2	IC50 value (μM)
2	2-pyridine	Phenhexyl	0.002
3	Hydrogen	Biphenylethyl	0.18
6	CN	Biphenylethyl	0.001
7	COOH	Biphenylethyl	0.02
14	2-pyridine	Biphenylethyl	0.0007
17	6-piconilic acid	Biphenylethyl	0.006
23	6-(1H-tetrazol-5-yl)pyridine-2-yl	Phenoxyphenethyl	0.1
30	Hydrogen	Phenhexyl	2.5
33	Cyanide	Phenhexyl	0.0065
34	COOH	Phenhexyl	0.002
40	6-piconilic acid	Phenhexyl	0.1
44	6-(1H-tetrazol-5-yl)pyridine-2-yl	Phenhexyl	0.5
45	Hydrogen	Phenoxyphenethyl	0.5
48	Cyanide	Phenoxyphenethyl	0.005
49	COOH	Phenhexyl	0.08
54	2-pyridine	Phenhexyl	0.002
56	6-piconilic acid	Phenhexyl	0.02
59	Hydrogen	(phenoxymethyl)phenethyl	0.27
62	Cyanide	(phenoxymethyl)phenethyl	0.002
63	COOH	(phenoxymethyl)phenethyl	0.05
68	2-pyridine	(phenoxymethyl)phenethyl	0.002
70	6-piconilic acid	(phenoxymethyl)phenethyl	0.04
74	6-(1H-tetrazol-5-yl)pyridine-2-yl	(phenoxymethyl)phenethyl	0.18

Table2.Structure and biological activity data of 5-(pyridin- 2-yl)oxazole motif derivative analogues used in QSAR analysis

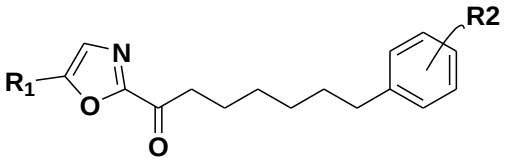

Compound	Substituents R1	Substituents R2	IC50 value (μM)
5e	2-pyridyl	2-pyridyl	0.03
5f	2-pyridyl	3-pyridyl	0.02
5gg	2-pyridyl	2-Cl	0.02
5hh	2-pyridyl	3-Cl	0.002
5ii	2-pyridyl	4-Cl	0.03
5j	2-pyridyl	2-OCH3	0.01
5k	2-pyridyl	3-OCH3	0.02
5l	2-pyridyl	4-OCH3	0.02
11a	2-pyridyl	CH2	0.001
11g	2-pyridyl	NH	0.005
11h	2-pyridyl	CH2	0.003
11i	2-pyridyl	S	0.002

Preparation of data set and reduction of data

Molecular descriptors are mostly used to investigate the structural information of all chemical structures and their related substituents and to get a good and predicted QSAR model. TSAR was used to compute over 200 molecular descriptors. It is a comprehensive analytic software for the interactive examination of quantitative structure-activity association. Since TSAR's worksheet included many numerical descriptors for molecular structure. Molecular characteristics, indices, VAMP parameters, and atom counts were considered in the computed descriptors.[20]

The training and testing sets comprised 35 compounds of α-ketooxazole derivatives. The expected values were found in the training and test sets, which included 24 and 11 compounds. MLR, PLS, and FFNN were used for model construction to perform external validation on training set molecules. It was also verified that the produced models had been internally validated.

Descriptors' viability is mostly examined throughout the data reduction phase. Data were first subjected to pair- and step-wise correlation analysis. Large numbers of descriptive terms with strongly correlated properties lead to a model with a poor predictability. When the correlation coefficient between two descriptors is more than 0.5, it indicates a strong association between the two and a lesser association with biological activity. Then it explicitly states that keeping that descriptor has no utility; therefore, it was removed while the other was maintained. This procedure was repeated until strongly associated descriptors for biological activity were found. Using three distinct molecular descriptors, Kier chi 5 ring index, VAMP heat of formation (whole molecule), and VAMP LUMO (whole molecule) were retrieved.

Development of models

Linear Regression Analysis

MLR and PLS were used to estimate the association between biological activity and statistically analysed physicochemical descriptors. The MLR model was quantified and predicted using x-variables (independent variables) and y-variable (dependent variables). Because it represents the connection between independent and dependent variables, MLR stands alone in the domain of regression analysis in the QSAR technique. The MLR equation exposes the relationship behaviour of descriptors with ki values, which aids in better understanding drug-receptor binding interactions and the development of novel chemical entities. The optimal model was chosen using statistical metrics like conventional regression coefficient (r^2), the standard error of estimation (SE), and Fischer's ratio (F). PLS has been suggested as an alternate method for increasing the amount of data in each model while avoiding the problem of over-fitting.[21]As with MLR, the findings of PLS regression may be utilized with more than one dependent variable[19] to verify or reconfirm the model. The leave-one-out approach was used to conduct cross-validation on the suggested model.

Non-linear regression analysis

FFNN (Feed Forward Neural Network) is a kind of ANN (Artificial Neural Network) that relies on only three basic building blocks: output, input, and hidden nodes. The information in the network only flows in one direction, from input nodes to output nodes through hidden nodes. Two modifications were made to the FFNN model: first, the proportion of data removed from prediction and second, the number of nodes in each hidden layer was changed. The best model revealed the closest and most applicable test RMS fit as well as training set RMS fit values. Correlation graphs show the relationship between descriptors and biological activity (IC_{50} values).

A relevant pharmacokinetic profile (ADME) was also found in these inhibitors. Lipinski's "rule of five" was applied to the complete data set. Christopher A. Lipinski introduced the rule in 1997 because most pharmaceutical medications are small and lipophilic compounds[22]. To be drug-like, molecules having a log p (>5), hydrogen bond acceptors (>10), molecular weight (>500), and hydrogen bond donors (>5) must have low adsorption or permeation, according to this criterion.[22,23] This rule outlines the molecular characteristics of medicine that are significant for its pharmacokinetics in the human body. Table 3 shows the calculated results of Lipinski's rule of five, which was considered.

Table 3. Values of calculated parameters for Lipinski's rule of five

Compound	ADME weight (Whole molecule)	ADME H bond acceptors	ADME H bond donors	ADME Log P Whole molecule	ADME Rotatable Bond	ADME violations
1	334.45	4	0	4.0422	9	2
2	277.34	3	0	4.1407	5	0
3	335.44	5	0	3.9848	9	1

4	335.44	5	0	4.1952	9	1
5	368.89	4	0	4.5602	9	2
6	368.89	4	0	4.5602	9	2
7	368.89	4	0	4.5602	9	2
8	364.48	5	0	3.7895	10	1
9	364.48	5	0	2.7895	10	1
10	364.48	5	0	3.7895	10	1
11	302.35	4	0	3.7699	5	0
12	321.35	5	1	3.6033	6	0
13	384.46	5	0	4.9809	8	0
14	369.45	4	1	4.5693	7	0
15	368.46	4	0	4.5377	7	1
16	386.49	4	0	4.2293	7	1
17	354.43	4	0	4.1414	6	1
18	398.44	6	1	4.774	7	0
19	438.48	8	1	4.4509	8	0
20	257.36	3	0	4.0415	8	0
21	282.37	4	0	3.6707	8	0
22	301.37	5	1	3.5041	9	1
23	378.46	6	1	4.6748	10	1
24	402.5	7	1	4.6071	10	1
25	293.34	4	0	3.8853	6	0
26	318.35	5	0	3.5145	6	0
27	337.35	6	1	3.3479	7	0
28	370.43	5	0	4.886	7	0
29	414.44	7	1	4.5186	8	0
30	307.37	4	0	3.9802	7	0
31	332.38	5	0	3.6094	7	0
32	351.38	6	1	3.4428	8	0
33	384.46	5	0	4.9809	8	0
34	428.47	7	1	4.6135	9	1
35	422.48	7	1	4.7063	7	0

Results and discussion

Linear regression analysis

The QSAR equations were derived using MLR and PLS. After reducing the data, we extracted three descriptors that are independent and could be utilized to design a regression model.

Outliers in QSAR may be relevant and interesting, particularly when observed biological activity exceeds the model's prediction (higher residual value). Outliers may occur for various reasons, including incorrect parameter value computation, an insufficient mathematical model, a lack of specific descriptors to define the QSAR for the whole compound, or a distinct mode of mechanism. The regression line of the equation was used to find two outliers (22 and 32). The statistical properties of the training set, such as LOO r^2cv and correlation coefficient *r,* were dramatically enhanced once these chemicals were removed from the training set. As a result, these compounds were finally removed from the training set, and MLR and PLS models for the remaining 42 compounds were developed. Equation-1 represents the best QSAR models (MLR & PLS) produced, with excellent values of $\mathbf{r^2cv}$ and r for the training set.

Equation 1 (MLR)

Y= 28.610481*X1 – 0.014945738*X2 + 1.58566373*X3 – 3.5233698

Where X1 is kierchi 5 (ring index), X2 is VAMP heat of formation (whole molecule), X3 is VAMP LUMO (whole molecule)

Performing MLR on training set compounds with the three selected descriptors that shows gradually increment in statistical values, were shown in Table 4and satisfactory r^2values of (training and test) confirms the robustness of the model as in Figure 1.

Table 4. Statistical tests and their values obtained after performing MLR analysis

ANALYSIS. Statistical tests	Values
s value	0.406483
F value	34.2924
Regression coefficient, r	0.922545
r^2	0.849
Cross validation, r^2 (cv)	0.802496

Results obtained from conventional MLR were checked with PLS analysis using same data set. PLS model (equation-2) complemented the MLR model in terms of model soundness (r^2) and predictability (r^2cv).

Equation 2 (PLS)

Y = 26.130547*X1- 0.013677232*X2 + 1.7142184*X3- 3.0601757

Where X1 is kierchi 5 (ring index), X2 is VAMP heat of formation (whole molecule), X3 is VAMP LUMO (whole molecule)

Table 5 illustrates the results of performing PLS on the training set compounds with the three chosen descriptors, which indicate a continuous increase in statistical values, and good r^2 values of (test and training) validate the model's resilience, as shown in Figure 2.

Table5.Statistical tests and their values obtained after performing PLS analysis

ANALYSIS. Statistical tests	Values
s value	1.1556
r^2	0.800
Cross validation, r^2 (cv)	0.80363

Feed forward neural network analysis

FFNN has been used on a dataset of constructed models, and it has performed on data sets with 45 percent of the data on three inputs, two hidden nodes, and one output. FFNN's r^2=0.857 (training) values are displayed in Table 6 and Figure 3, and the plot dependencies were also analysed, with FFNN showing a positive performance (Figures 4, 5, and 6).

Table6. Details of FNN

Summary of FFNN	
Net configuration	3-2-1
Test RMS fit	0.143874
No. of cycles	1144
Best RMS fit	0.095023

Test set prediction

It was also tested using test sets of substances eliminated from the model's construction. A similar approach was used for the test and training sets of compounds. The r^2 values of PLS= 0.763 and MLR= 0.800 obtained for the test set show that the created model has a strong predictive capacity. With the same external test set, we evaluated the MLR predictability to that of FFNN and found that the r^2 was comparable in both cases (0.807).

Tables 7 and 8 provide the actual and predicted activity from MLR, FFNN, and PLS analyses for the training and test sets of chemicals, respectively, and Figure 1-3 shows the related graphs.

The three strongly correlated parameters are retained on the TSAR sheet and are then utilized to construct a regression equation and analysed for their respective effects on the compound activity (Table 9). As a result, all of the values of t-test, Covariance SE, and Jacknife SE in Table 10 are significant for the best model, indicating the relevance of each descriptor.

Table 7. Actualand predicted activity data obtained from linear and non-linear analysis for training set compounds

Compounds No.	Actual Value (Log 1/c)	Predictive value		
		MLR	PLS	FNN
1	-2.699	-2.01303	-2.15198	-1.89536
2	-0.74473	-0.71373	-0.90289	-0.24379
3	-1.52288	-2.14024	-2.13199	-1.93261
4	-1.69897	-2.18042	-2.16297	-2.18271

5	-1.69897	-1.91714	-1.93087	-1.7697
6	-2.69897	-1.93719	-1.95349	-1.89378
7	-1.52288	-1.94615	-2.06023	-1.92313
17	-3.1549	-2.78824	-2.74341	-3.17635
18	-2.2218	-2.02348	-2.04701	-1.85812
19	-1	-0.71207	-0.15107	-1.17112
20	0.39794	0.08016	-0.0594	0.238963
21	-2.18709	-2.39057	-2.32748	-2.1736
24	-0.30103	-0.27017	-0.23816	-1.39119
25	-0.30103	-0.46201	-0.79839	-0.15728
26	-2.30103	-2.84265	-2.85264	-2.62772
28	-2.69897	-2.46557	-2.42144	-2.65383
29	-1.69897	-1.70679	-1.82972	-1.74445
30	-0.56864	-0.28296	-0.28503	0.008884
31	-2.699	-2.64176	-2.59108	-2.48083
33	-2.69897	-2.34762	-2.41081	-2.34762
34	-1.39794	-1.58815	-1.75122	-1.58815
35	-0.74473	-1.03377	-1.06125	-1.03377

Table 8. Actual and predicted activity data obtained from linear and non-linear analysis for test set of compounds

Compounds No.	Actual Value (Log 1/c)	Predictive value		
		MLR	PLS	FNN
8	-2	-1.79428	-1.83535	-1.88466
9	-1.69897	-1.78197	-1.82554	-1.82376
10	-1.69897	-1.78151	-1.82596	-1.8271
11	-3	-2.73336	-2.74232	-3.00641
12	-1.69897	-1.4605	-1.4845	-1.03488
13	-3	-2.37461	-2.40013	-2.96487
14	-2.30103	-2.81993	-2.80753	-2.35466
15	-2.52288	-2.67148	-2.7192	-2.67114
16	-2.69897	-2.78775	-2.75328	-2.54584
23	-1	-1.30008	-1.29423	-0.99143
27	-1.09691	-1.21123	-1.19299	-0.99573

Table 9. Correlation matrix showing-correlation between biological activity and parameters

	Log value	Kier Chi5 (ring index)	VAMP Heat of Formation (Whole Molecule)	VAMP LUMO (Whole Molecule)
Log value	1	0.51427	-0.047407	0.23698
Kier Chi5 (ring index)	0.51427	1	0.66335	-0.28366
VAMP Heat of Formation (Whole Molecule)	-0.047407	0.66335	1	-0.11892
VAMP LUMO (Whole Molecule)	0.23698	-0.28366	-0.11892	1

Table 10. t-test values, Jacknife SE and Covariance SE for the selected descriptors

	t-test value	Jacknife SE	Covariance SE
Kier Chi5 (ring index)	8.9773	2.7472	2.7938
VAMP Heat of Formation (Whole Molecule)	-6.0945	0.0027518	0.001723
VAMP LUMO (Whole Molecule)	4.9101	0.33069	0.35391

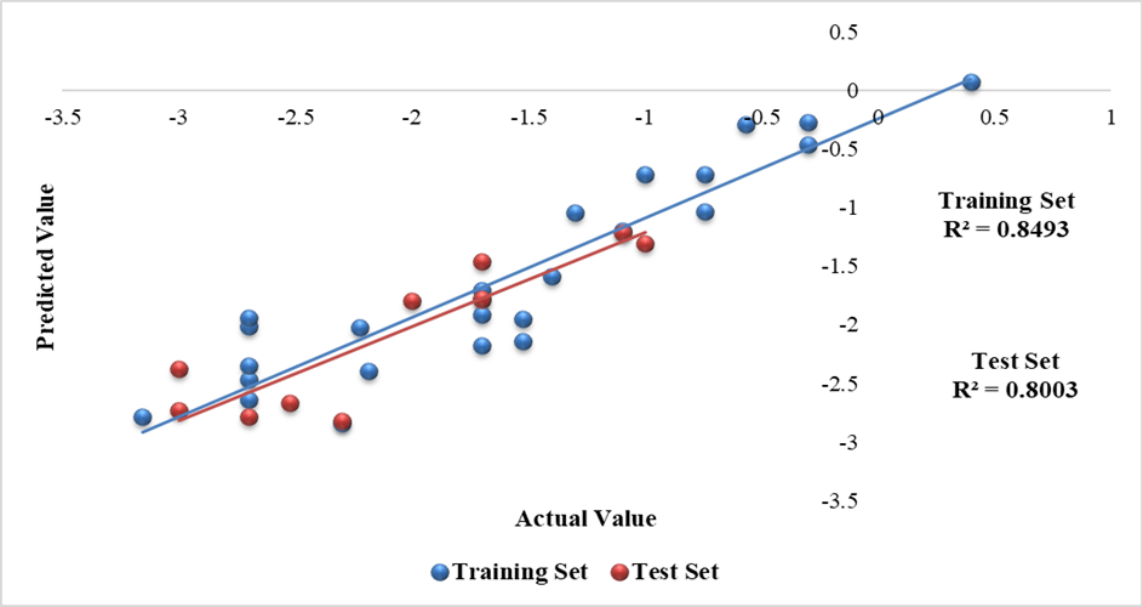

Figure1.Plot of actual versus predicted activity for the training set and test set of compounds derived from MLR analysis

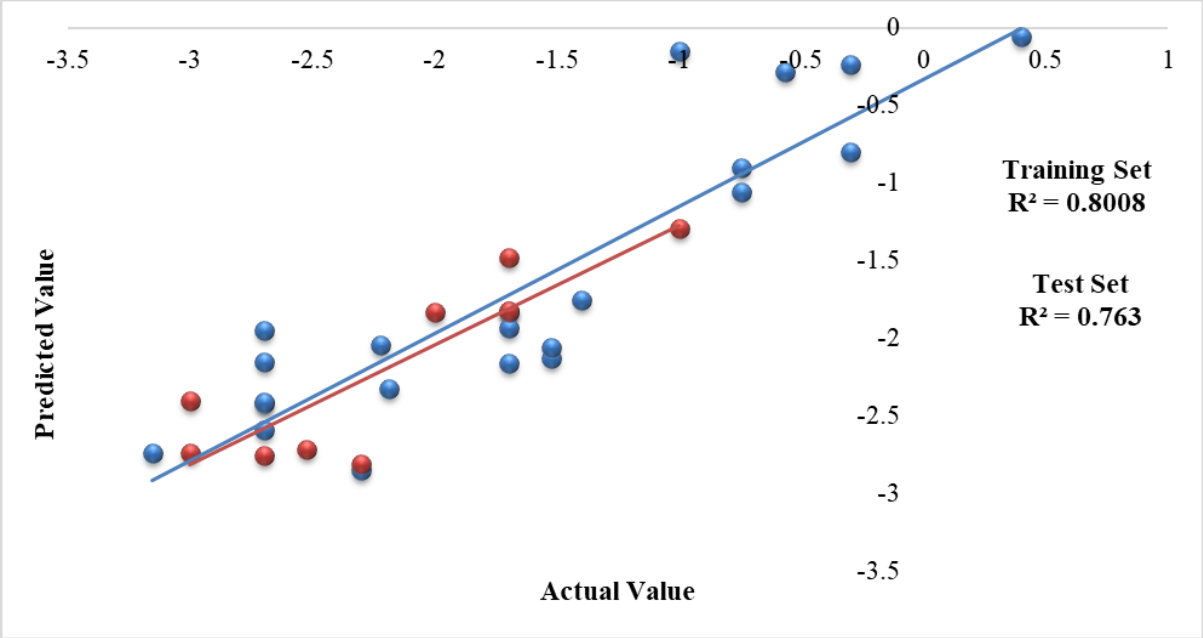

Figure2.Plot of actual versus predicted activity for the test set of compounds derived from PLS analysis

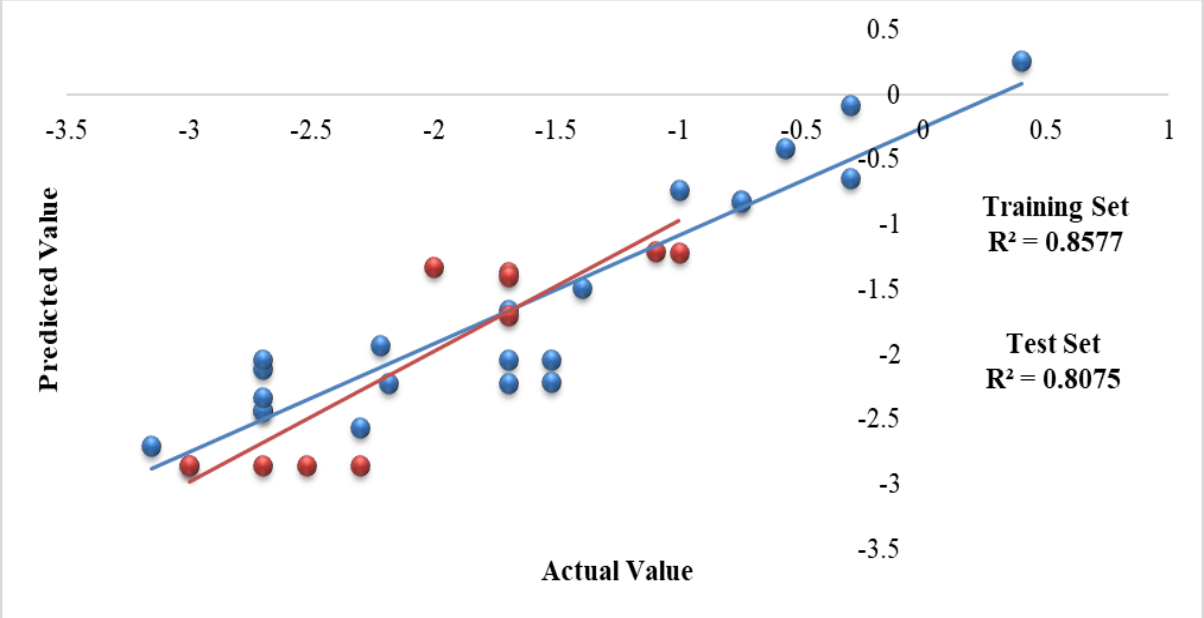

Figure3:Plot of actual versus predicted activity for the training set and test set of compounds derived from FNN analysis

Interpretation of descriptors entered

The three parameters Kier chi 5 ring index, VAMP heat of formation (whole molecule), VAMP LUMO (whole molecule) showing high correlation with biological activity are utilized to create regression equations, which were then analysed for their relative influence on compound activity.

Kier chi 5 ring index

As shown by the correlation matrix and t-value, the Kier Chi 5 ring index (whole molecule) was a key descriptor in characterizing the biological activity of urea-based derivatives. First developed by Randic, the Kier Chi 5 ring index has since been revised by Kier and Hall. It depicts different series using the "order" and "subgraph" types. A chi-index is a weighted computation of a known subgraph type like a cluster (C), path (P), ring (CH), and path/cluster (PC). The description shows many characteristics of atom connectivity in a molecule. In addition, it enables us to study the substitution pattern in benzene rings and the number of branching rings. According to our analysis, the Kier chi 5 ring index descriptor is positively linked to permeability (Figure 4) because it reflects structural complexity, such as the ring's size and heteroatom content (Kierchi 5).Complexity may be seen in both the most and least active compounds of the substance.[24]

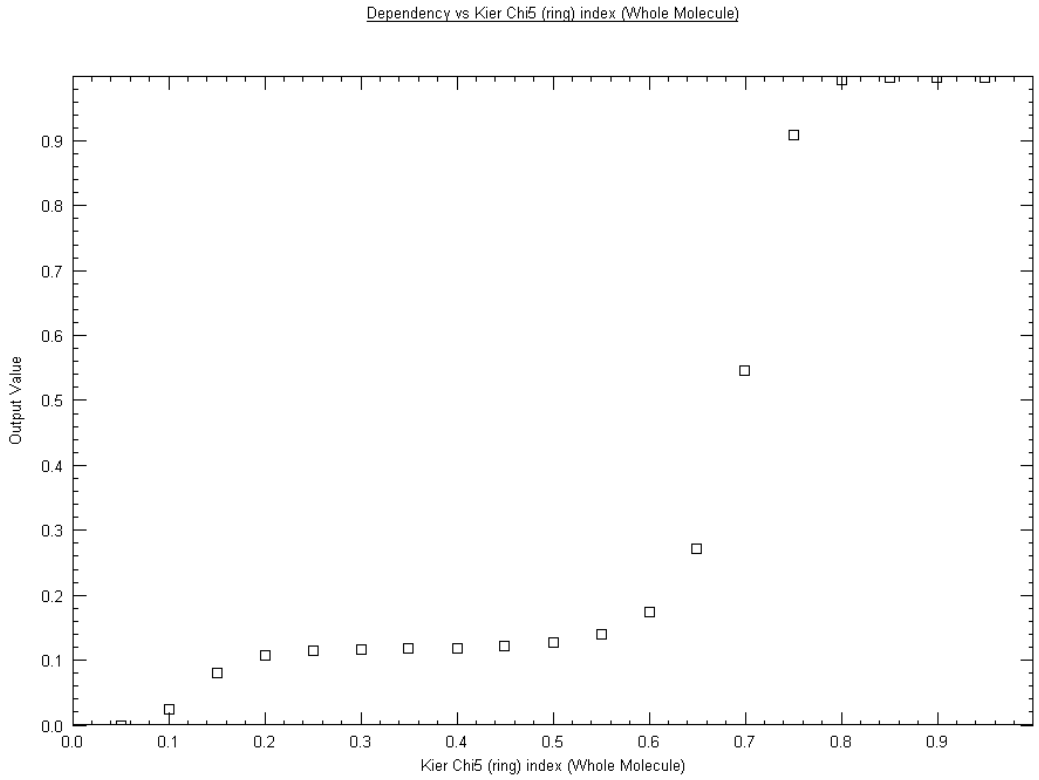

Figure4. Dependency plot between biological activity and kier chi 5 ring index (whole molecule)

VAMP heat of formation (Whole molecule)

The enthalpy of creating a molecule from its component atoms is a measure of a molecule's thermal stability. The MNDO semi-empirical molecular orbital approach of DWAR is used to compute this descriptor. This is the most rigorous quantum chemical approach known for QSAR and has a broad variety of applications in conformational analysis, chemical reaction, and intermolecular modeling.In our study (Figure 5), VAMP heat of formation (whole molecule) is negatively associated with biological activity. Thus, with a reduction in VAMP heat of molecule production, the biological activity would increase.[25,26]

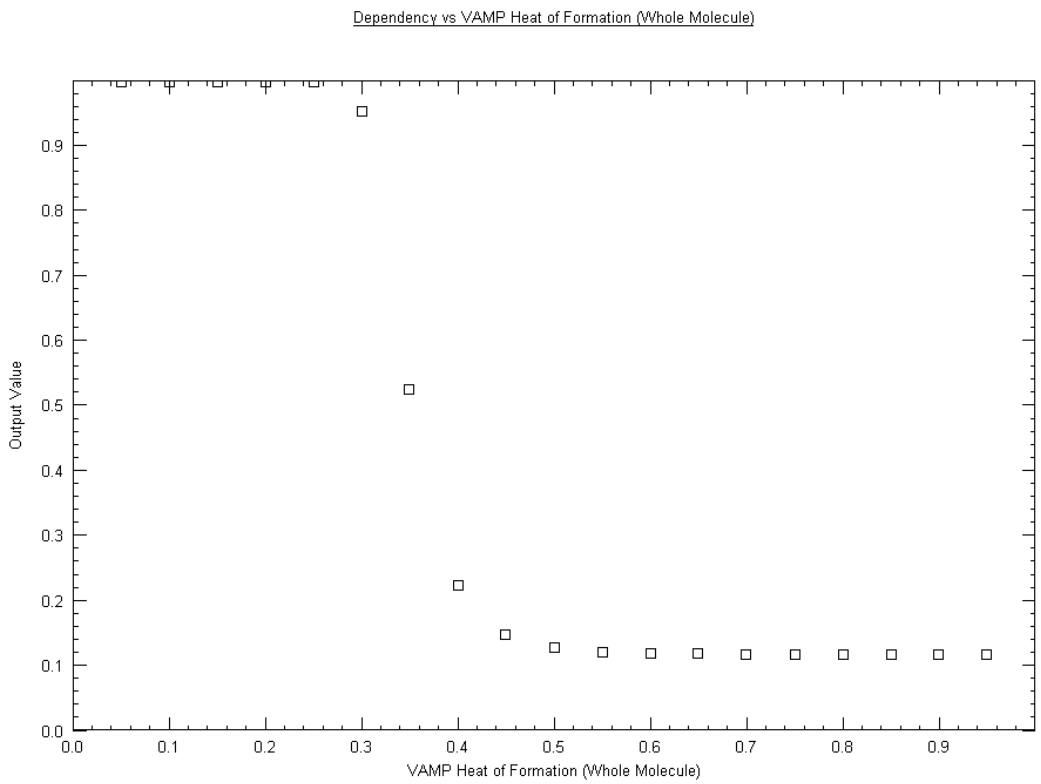

Figure5. Dependency plot between biological activity and VAMP Heat of formation (whole molecule)

VAMP LUMO (Whole molecule)

The lowest energy level of a molecule containing no electrons is LUMO (lowest unoccupied molecular orbital). It has a significant impact on the characteristics and reactivity of molecules. LUMO is where electron pairs are received when a molecule functions as a Lewis acid (an electron-pair acceptor) during bond formation. The LUMO descriptor should quantify a molecule's ability to receive electrons since molecules with low LUMOs have better ability to accept electrons in comparison to molecules with high LUMOs. It has a negative correlation with activity. Thus, molecules that show low LUMO should show good anti-Alzheimer activity. In the FFNN dependency graphs of the tri-parametric model (Figure 6), log IC decreases with the increase in values of the Vamp LUMO (whole molecule). Our PLS and MLR models show that the decreasing trend is in good agreement with our findings (the descriptors have positive coefficients).[27]

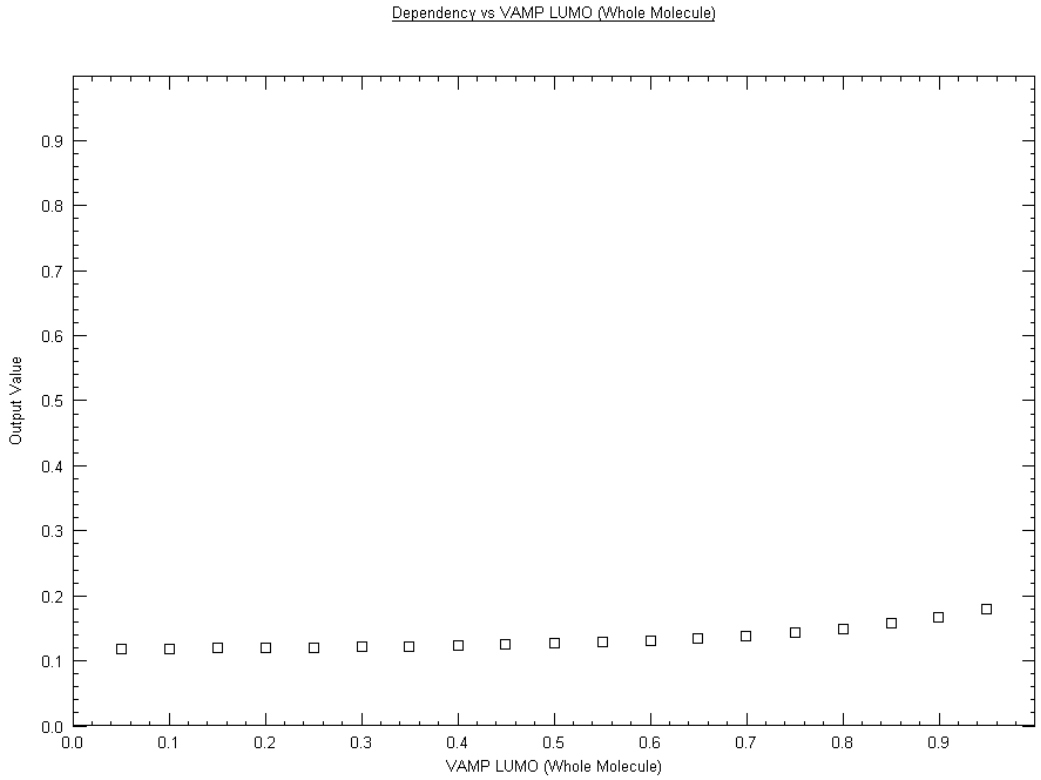

Figure6. Dependency plot between biological activity and VAMP LUMO (whole molecule)

Conclusion

A successful QSAR research was conducted on a series of α-ketooxazole compounds that inhibit FAAH. MLR, FFNN, and PLS analyses were done on the model, and the findings were quite predictive and demonstrated similar results and some valuable parameter information. The remaining compound descriptors encode the shape, polarity, and lipophilic architecture of α-ketooxazole and are regarded as key contributors to their biological characteristics according to the conventional QSAR models described in this study.

References

1. Hardy J, Selkoe DJ. The amyloid hypothesis of Alzheimer's disease: Progress and problems on the road to therapeutics. Science (80-)**2002**;297(5580):353-356.
2. Buée L, Bussière T, Buée-Scherrer V, Delacourte A, Hof PR. Tau protein isoforms, phosphorylation and role in neurodegenerative disorders. Brain Res Rev. **2000**; 33(1):95-130.
3. Aso E, Ferrer I. Cannabinoids for treatment of alzheimer's disease: Moving toward the clinic. Front Pharmacol. **2014**;5:1-11.
4. Giacobini E. Cholinergic function and Alzheimer's disease. Int J Geriatr Psychiatry. **2003**;18:1-5.
5. Darvesh S, Hopkins DA, Geula C. Neurobiology of butyrylcholinesterase. Nat Rev Neurosci. **2003**;4(2):131-138.
6. Greig NH, Utsuki T, Ingram DK, et al. Selective butyrylcholinesterase inhibition elevates brain acetylcholine, augments learning and lowers Alzheimer β-amyloid peptide in rodent. Proc Natl Acad Sci U S A. **2005**;102(47):17213-17218.

7. Sharma A, Piplani P. Understanding the quantitative structure-activity relationship of acetylcholinesterase inhibitors for the treatment of Alzheimer's disease. J Theor Comput Chem. **2015**;14(6):1-27.
8. Tanaka M, Yagyu K, Sackett S, Zhang Y. Anti-Inflammatory effects by pharmacological inhibition or knockdown of fatty acid amide hydrolase in BV2 microglial cells. Cells. **2019**;8(5):491.
9. Mphahlele MJ, Gildenhuys S, Agbo EN. In vitro evaluation and docking studies of 5-oxo-5h-furo[3,2-g]chromene-6-carbaldehyde derivatives as potential anti-alzheimer's agents. Int J Mol Sci. **2019**;20(21).
10. Koppel J, Davies P. Targeting the endocannabinoid system in Alzheimer's disease. J Alzheimer's Dis. **2008**;15(3):495-504.
11. Núñez E, Benito C, Tolón RM, Hillard CJ, Griffin WST, Romero J. Glial expression of cannabinoid CB2 receptors and fatty acid amide hydrolase are beta amyloid-linked events in Down's syndrome. Neuroscience. **2008**;151(1):104-110.
12. C B, RM T, AI C, et al. β-Amyloid exacerbates inflammation in astrocytes lacking fatty acid amide hydrolase through a mechanism involving PPAR-α, PPAR-γ and TRPV1, but not CB_1 or CB_2 receptors. Br J Pharmacol. **2012**;166(4):1474-1489.
13. Jain S, Bisht A, Verma K, Negi S, Paliwal S, Sharma S. The role of fatty acid amide hydrolase enzyme inhibitors in Alzheimer's disease. Cell Biochem Funct. Published online December 21, **2021**.
14. Han SH, Shim S, Kim MJ, et al. Long-term culture-induced phenotypic difference and efficient cryopreservation of small intestinal organoids by treatment timing of Rho kinase inhibitor. World J Gastroenterol. **2017**;23(6):964-975.
15. Dearden JC, Hewitt M, Geronikaki AA, Garibova TL, Macaev FZ, Voronina TA. QSAR investigation of new cognition enhancers. QSAR Comb Sci. **2009**;28(10):1123-1129.
16. Roy K. On some aspects of validation of predictive quantitative structure-activity relationship models. Expert Opin Drug Discov. **2007**;2(12):1567-1577.
17. Hardouin C, Kelso MJ, Romero FA, et al. Structure-activity relationships of α-ketooxazole inhibitors of fatty acid amide hydrolase. J Med Chem. **2007**;50(14):3359-3368.
18. Lira R, Johnson DS. Optimization of α-ketooxazole inhibitors of fatty acid amide hydrolase. Chemtracts. **2008**;21(5):184-192.
19. Paliwal S, Narayan A, Paliwal S. Quantitative structure activity relationship analysis of dicationic diphenylisoxazole as potent anti-trypanosomal agents. QSAR Comb Sci. **2009**;28(11-12):1367-1375.
20. Paliwal S, Seth D, Yadav D, Yadav R, Paliwal S. Development of a robust QSAR model to predict the affinity of pyrrolidine analogs for dipeptidyl peptidase IV (DPP-IV). J Enzyme Inhib Med Chem. **2011**;26(1):129-140.
21. Kubinyi H. Evolutionary variable selection in regression and PLS analyses. J Chemom. **1996**;10(2):119-133.
22. Lipinski CA. Lead- and drug-like compounds: The rule-of-five revolution. Drug Discov Today Technol. **2004**;1(4):337-341.
23. Lipinski CA, Lombardo F, Dominy BW, Feeney PJ. Experimental and computational approaches to estimate solubility and permeability in drug discovery and development settings. Adv Drug Deliv Rev. **2012**;64:4-17.

24. Kesar S, Paliwal SK, Mishra P, Chauhan M. Quantitative structure-activity relationship analysis of selective rho kinase inhibitors as neuro-regenerator agents. Turkish J Pharm Sci. **2019**;16(2):141-154.
25. Agarwal A, Paliwal S, Mishra R. Molecular Modeling Studies of RNA Polymerase II Inhibitors as Potential Anticancer Agents. Internatinal J Adv Pharmacy, Biol Chem. **2013**;2(2):338-345.
26. Madan K, Verma AN, Paliwal SK, Yadav D, Sharma S, Sharma M. Pharmacophore Modeling and Database Mining to Identify Novel Lead Compounds Active Against the Disease Stage of Trypanosomiasis in the Central Nervous System Background. **2021**;(1):1-11.
27. Dwivedi N, Mishra BN, Katoch VM. 2D-QSAR model development and analysis on variant groups of anti -tuberculosis drugs. Bioinformation. **2011**;7(1):82-90.